scientific reports

OPEN

Dynamic analysis of a Caputo fractional-order SEIR model with a general incidence rate

Shenghu Xu✉ & Yanhui Hu

This study develops a fractional-order SEIR model with asymptomatic infections and memory effects, introducing a generalized incidence rate to better reflect the nonlinear characteristics of transmission. The Caputo fractional derivative is used to capture memory effects and non-locality, dynamically adjusting the order to adapt to complex processes, improving accuracy and fitting. Based on Lyapunov functions, we rigorously prove that the disease-free equilibrium is globally asymptotically stable when $R_0 < 1$, and the endemic equilibrium is globally stable when $R_0 > 1$. Sensitivity analysis identifies key factors influencing disease spread and control. Numerical simulations validate the theoretical results and demonstrate the advantages of the fractional-order model in capturing epidemic dynamics, which traditional integer-order models fail to capture such dynamics. This study contributes to more accurate disease modeling and provides insights for optimizing control strategies for complex infectious diseases.

Infectious diseases have posed a considerable challenge throughout history[1,2], driving ongoing research. From smallpox outbreaks in ancient Egypt[3] to the Black Death[4] and cholera pandemics[5] of the 19th century, more recently SARS and COVID-19 outbreaks, each event has left a lasting impact on human society. These crises have also spurred advancements in science, technology, and public health. In 1796, Edward Jenner developed the first effective vaccine, marking the beginning of modern vaccine development and ultimately leading to global smallpox eradication in the 20th century. Similarly, Louis Pasteur developed vaccines for rabies and anthrax and pioneered research improving food safety and sanitation practices.

Infectious disease models[6,7] have undergone several significant stages of development. British researchers John Graunt and William Farr used statistical methods to analyze disease trends in the 17th century. By the early 20th century, mathematical modeling of infectious disease became more systematic. In 1927, British mathematicians Kermack[8] and McKendrick introduced the SIR model, laying the foundation for modern infectious disease modeling. Building on this, infectious disease models expanded and improved in the second half of the 20th century. The SEIR model[9] was developed to account for diseases where individuals may be infected but not yet contagious. In addition to fractional-order modeling methods, other mathematical tools have also been widely applied in complex system modeling in recent years, including Bayesian games[10], Boolean control networks[11], fractal mappings[12], and discrete system stability analysis[13]. These methods have been applied in various fields and may provide new perspectives for future research in epidemiological dynamics.

School of Mathematics and Information Science, North Minzu University, Yinchuan 750021, Ningxia, People's Republic of China. ✉email: xuluck2001@163.com

More recently, Wang et al.[14] further subdivided the infected compartment into symptomatic and asymptomatic individuals, allowing for more accurate representation of diseases with asymptomatic transmission. Wang et al.[14] proposed the SEIR model as follows:

$$
\begin{cases}
\dfrac{dS}{dt} = \Lambda - \beta S(I_1 + I_2) - \mu S, \\[2mm]
\dfrac{dE}{dt} = \beta S(I_1 + I_2) - (\epsilon + \mu)E, \\[2mm]
\dfrac{dI_1}{dt} = p\epsilon E - (\mu + \alpha + r_1)I_1, \\[2mm]
\dfrac{dI_2}{dt} = q\epsilon E - (\mu + \alpha + r_2)I_2, \\[2mm]
\dfrac{dR}{dt} = r_1 I_1 + r_2 I_2 - \mu R,
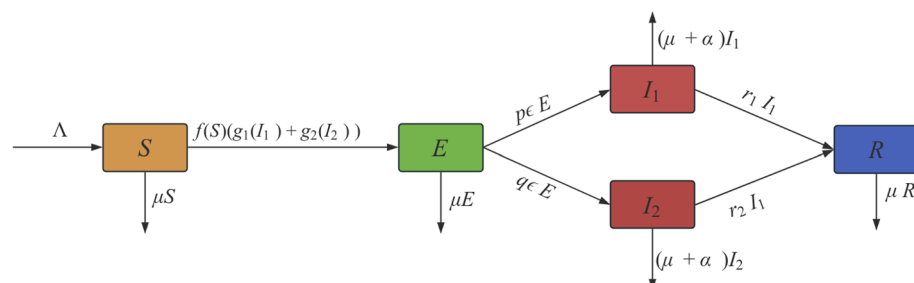\end{cases}
\tag{1}
$$

where S denotes susceptible individuals, E stands for exposed individuals, $I_1(t)$ is the number of infectious individuals, who are diagnosed and symptomatic, $I_2(t)$ is the number of the infectious individuals, who are diagnosed but asymptomatic, and R indicates recovered individuals. The parameter Λ represents the recruitment rate of susceptible individuals, and β is the transmission rate through contact. μ is the natural mortality rate, and ϵ is the diagnosis rate. The proportion of symptomatic individuals among all diagnosed cases is denoted by p, and q is the proportion of asymptomatic individuals. α stands for the mortality rate due to the disease. Lastly, r_1 and r_2 represent the recovery rates of symptomatic and asymptomatic individuals, respectively. It is assumed that the parameters Λ and μ are positive, while the parameters $\beta, \epsilon, p, q, \alpha, r_1$, and r_2 are non-negative, with the condition that $p + q = 1$.

"*The asymptomatic ratio $q = 0.3166$ aligns with empirical COVID-19 data[14], where 30–40% of infections are asymptomatic. This assumption increases R_0 by 18% compared to models ignoring I_2.*" For more information on the model, we refer interested readers to[14] and the reference there in.

Based on the model in[14], we introduce the SEIR model with general incidence rate, The model can be described as follows, and we design a flowchart based on the general incidence rate model (Fig. 1).

$$
\begin{cases}
\dfrac{dS}{dt} = \Lambda - f(S)(g_1(I_1) + g_2(I_2)) - \mu S, \\[2mm]
\dfrac{dE}{dt} = f(S)(g_1(I_1) + g_2(I_2)) - (\epsilon + \mu)E, \\[2mm]
\dfrac{dI_1}{dt} = p\epsilon E - (\mu + \alpha + r_1)I_1, \\[2mm]
\dfrac{dI_2}{dt} = q\epsilon E - (\mu + \alpha + r_2)I_2, \\[2mm]
\dfrac{dR}{dt} = r_1 I_1 + r_2 I_2 - \mu R.
\end{cases}
\tag{2}
$$

Fractional calculus[15–17] expands upon traditional integer-order calculus, concentrating on the investigation of derivatives and integrals of arbitrary real or complex orders. Although the concept of fractional derivatives was first introduced by Leibniz in 1695, the field did not advance rapidly at that time. Nonetheless, in recent years, fractional calculus has emerged as a highly active research area[18–21] propelled by its growing application to practical problems, particularly in fields such as nonlinear dynamics, control theory, signal processing, and quantum mechanics. Compared to traditional calculus, fractional calculus enhances flexibility and precision in describing complex physical phenomena and system behaviors[22–25,31]. Researchers have studied Lyapunov functions for fractional-order systems and derived key fractional-order inequalities, which play a crucial role in proving the global stability of various fractional order models[26,27]. They have also examined the incorporation of a fractional order SEIR model without asymptomatic infective individuals. The Caputo fractional derivative

Fig. 1. The flowchart of SEIR with general incidence rate.

effectively describes the long-term dynamics of disease, such as incubation periods and immune decay. Compared to other types of fractional derivatives, the Caputo derivative is more applicable to epidemiological modeling, particularly due to its compatibility with traditional integer-order differential equations. Memory effects arise from the non-local nature of fractional derivatives, where past states influence current dynamics through a power-law kernel $(t-u)^{-\gamma}$. Therefore, we propose integrating the fractional Caputo derivative into the SEIR model with general incidence rate and asymptomatic infective individuals

$$\begin{cases} {}^{C}_{0}D^{\gamma}_{t}S(t) = \Lambda - f(S)(g_1(I_1) + g_2(I_2)) - \mu S, \\ {}^{C}_{0}D^{\gamma}_{t}E(t) = f(S)(g_1(I_1) + g_2(I_2)) - (\epsilon + \mu)E, \\ {}^{C}_{0}D^{\gamma}_{t}I_1(t) = p\epsilon E - (\mu + \alpha + r_1)I_1, \\ {}^{C}_{0}D^{\gamma}_{t}I_2(t) = q\epsilon E - (\mu + \alpha + r_2)I_2, \\ {}^{C}_{0}D^{\gamma}_{t}R(t) = r_1 I_1 + r_2 I_2 - \mu R, \end{cases} \tag{3}$$

where $\gamma \in (0, 1]$ and initial conditions

$$S(0) > 0, E(0) > 0, I_1(0) > 0, I_2(0) > 0, R(0) > 0. \tag{4}$$

Moreover, we assume that the functional response function $f(x)$ and $g_i(x)$ satisfies the following conditions:

(A_1): $f(0) = 0, f'(x) > 0$, for all $x \geq 0$.

(A_2): $g_i(0) = 0, g'_i(x) > 0$; $\frac{g_i(x)}{x}$ is non-increasing for all $x \geq 0, i = 1, 2$.

Condition A_1 ensures $f(S)$ increases with susceptible density, while condition A_2 captures the saturation effects via through the non-increasing term $g_i(I_i)/I_i$. This form not only includes the classic bilinear infection rate ($\beta SI, \beta > 0$), but also incorporates saturation effects($\frac{\beta SI}{1+\alpha I}, \beta, \alpha > 0$.), Crowley-Martin incidence rate ($\frac{\beta SI}{(1+aS)(1+bI)}, \beta, a, b > 0$.), sublinear incidence rate($\beta SI^p, \beta > 0, 0 < p < 1$.), and generalized saturation ($\frac{\beta S \cdot I}{1+\alpha I^{\gamma}}, \beta, \alpha > 0, \gamma \geq 1$.).

The generalized incidence rate function more accurately describes the changes in transmission caused by factors such as population size, behavioral changes, and asymptomatic individuals. In particular, asymptomatic individuals play an important role in transmission, which traditional linear models fail to capture effectively. By adjusting the transmission rates, the model can effectively simulate the effects of medical interventions and social distancing measures. By numerically simulating the adjustments of parameters β_1 and β_2, the model better adapts to different epidemic scenarios. For example, reducing the contact frequency of highly infectious groups can significantly reduce R_0, thereby effectively controlling the spread of the epidemic. The function enhances the model's adaptability to various transmission mechanisms, better fits real epidemic data, and provides strong support for public health decision-making, helping to formulate more precise control strategies.

Model (3) generalizes many special cases available in the literature[26,27]. The system (3) includes the following SEIR models:

- Model of Yang et al.[26] with $I_2 = 0$.
- Model of Almeida et al.[27] with $f(s) = s, g_1(I_1) = I_1$, and $I_2 = 0$

The references in[28–30] all study fractional-order SEIR models, which discuss the transmission processes of COVID-19, Ebola and H1N1/09 influenza. The above models are all SEIR models with bilinear infection rates. However, the model (3) with general incidence rate, brings a new difficulty if the nonlinear incidence rate combines with the effect of fractional-order derivative. *Recent studies [42,43] demonstrate Caputo models' efficacy in HIV-malaria co-infection dynamics, supporting our frameworks versatility.*

The organization of this paper is as follows: section "Preliminaries" provides the definitions and basic results of Caputo fractional calculus. Section "Well-posedness" conducts a qualitative analysis of the model. Section "Stability analysis" focuses on the dynamical analysis of the model. In section "Sensitivity analysis", we select common incidence functions for sensitivity analysis and provide control and prevention recommendations based on the model's results. In section "Numerical simulations", we present numerical simulations to verify the correctness of the theoretical findings and explore the memory and hereditary properties of the fractional-order model.

Preliminaries

In this section, some definitions and lemmas are provided.

Definition 2.1 [32]. For any integrable function $f : \mathbb{R}_+ \to \mathbb{R}$, the Riemann-Liouville fractional integral is defined as

$$I^{\gamma}_t f(t) = \frac{1}{\Gamma(\gamma)} \int_{t_0}^{t} (t-u)^{\gamma-1} f(u)\mathrm{d}u,$$

where $t_0 \leq t, 0 < \gamma < 1$.

Definition 2.2 [32]. The Caputo fractional derivative operator of the function f is defined as

$$
{}^{C}_{t_0}D^{\gamma}_t f(t) = \frac{1}{\Gamma(1-\gamma)} \int_{t_0}^{t} (t-u)^{-\gamma} \frac{\mathrm{d}}{\mathrm{d}u} f(u)\mathrm{d}u,
$$

where $0 < \gamma < 1$.

Definition 2.3 [32]. The two-parameters Mittag-Leffler function is defined as

$$
E_{\eta_1,\eta_2}(z) = \sum_{k=0}^{\infty} \frac{z^k}{\Gamma(k\eta_1 + \eta_2)}, \eta_1, \eta_2 > 0, z \in \mathbb{C}.
$$

In brief, let $E_{\eta_1}(z) := E_{\eta_1,1}(z)$.
The Laplace transform of the Caputo fractional derivative is given by

$$
\mathcal{L}\{{}^{C}_{0}D^{\gamma}_t g(t)\} = s^{\gamma} F(s) - \sum_{k=0}^{n-1} s^{\gamma-k-1} g^{(k)}(0), n < \gamma < n-1.
$$

The Laplace transform of the function $t^{\eta_2 - 1} E_{\eta_1,\eta_2}(\pm\lambda t^{\eta_1})$ can be expressed as

$$
\mathcal{L}[t^{\eta_2-1} E_{\eta_1,\eta_2}(\pm\lambda t^{\eta_1})] = \frac{s^{\eta_1 - \eta_2}}{s^{\eta_1} \mp \lambda},
$$

where $F(s) = \mathcal{L}(g(t))$.

Lemma 2.1 [33]. Consider the following fractional-order system

$$
{}^{C}_{t_0}D^{\gamma}_t g(t) = f(t, g(t)),
$$

with the initial condition $g(t_0) = g_{t_0}$ and $0 < \gamma < 1$. The condition for the local asymptotic stability of the equilibrium points of this system is that for every eigenvalue η_i of the Jacobian matrix $\frac{\partial f(t,y)}{\partial g}$, evaluated at the equilibrium points, it holds that $|\arg(\eta_i)| > \frac{\gamma\pi}{2}$.

Lemma 2.2 [22]. Let $\psi(t) \in C[0,\infty)$ satisfy ${}^{C}_{t_0}D^{\gamma}_t \psi(t) + b_1\psi(t) \leq b_2$, $\psi(0) = \psi_0$, where $0 < \gamma \leq 1$, and $b_1, b_2 \in \mathbb{R}$, with $b_1 \neq 0$. Then,

$$
\psi(t) \leq (\psi_0 - \frac{b_2}{b_1})E_{\gamma,1}(-b_1 t^{\gamma}) + \frac{b_2}{b_1},
$$

where $E_{\gamma,1}(\cdot)$ is a one parameter Mittag-Leffler function.

Lemma 2.3 [24]. Consider $u(t)$ be a real positive differentiable function. Then, for any $t \geq t_0$, $0 < \gamma \leq 1$, and $u^* > 0$, it follows that

$$
{}^{C}_{t_0}D^{\gamma}_t \Psi(u(t)) \leq \left(1 - \frac{g(u^*)}{g(u(t))}\right) {}^{C}_{t_0}D^{\gamma}_t u(t),
$$

where $\Psi(u) = \int_{u^*}^{u} \frac{g(s) - g(u^*)}{g(s)} ds$, the function g is a non-negative, differentiable, and strictly increasing on $\mathbb{R}^+$. Note that Ψ is positive on $\mathbb{R}^+ \backslash u^*$ with $\Psi(u^*) = 0$. In fact, Ψ is differentiable and

$$
\frac{d\Psi}{du} = 1 - \frac{g(u^*)}{g(u)}.
$$

Since g is a strictly increasing function, Ψ is strictly decreasing for $u < u^*$ and strictly increasing for $u > u^*$, where u^* represents the global minimum.

Well-posedness
Theorem 3.1 The system (3) with initial condition (4) has a unique solution.

$$
\Omega = \left\{ (S, E, I_1, I_2, R) \in \mathbb{R}^5_+ : S, E, I_1, I_2, R > 0, S + E + I_1 + I_2 + R \leq S_0 \right\}
$$

is positively invariant, where $S_0 = \frac{\Lambda}{\mu}$.

Proof Define

$$X(t) = \begin{pmatrix} S(t) \\ E(t) \\ I_1(t) \\ I_2(t) \\ R(t) \end{pmatrix}, \quad X_0 = \begin{pmatrix} S(0) \\ E(0) \\ I_1(0) \\ I_2(0) \\ R(0) \end{pmatrix},$$

and

$$h(X(t)) = \begin{pmatrix} h_1(X(t)) \\ h_2(X(t)) \\ h_3(X(t)) \\ h_4(X(t)) \\ h_5(X(t)) \end{pmatrix} = \begin{pmatrix} \Lambda - f(S)(g_1(I_1) + g_2(I_2)) - \mu S \\ f(S)(g_1(I_1) + g_2(I_2)) - (\epsilon + \mu)E \\ p\epsilon E - (\mu + \alpha + r_1)I_1 \\ q\epsilon E - (\mu + \alpha + r_2)I_2 \\ r_1 I_1 + r_2 I_2 - \mu R \end{pmatrix}.$$

The system with initial conditions can be expressed as follows

$$\begin{cases} {}^C_0 D^\gamma_t X(t) = h(X(t)), \\ \qquad X(0) = X_0. \end{cases}$$

Given conditions (A_1) and (A_2), we know that the Jacobian matrix $\frac{\partial h}{\partial x} = \frac{\partial(h_1, h_2, h_3, h_4, h_5)}{\partial(S, E, I_1, I_2, R)}$ is continuous on $\mathbb{R}^5_+$. Using Remark 1.2.1 from[34], it follows that h is locally Lipschitz continuous on $\mathbb{R}^5_+$. Moreover, applying Remark 3.8 from[35], we conclude that the system (3) with (4) has a unique solution.

To show the positivity of the solutions, we derive the following from system (3),

$$\left. {}^C_0 D^\gamma_t S(t) \right|_{S=0} = \Lambda \geq 0,$$
$$\left. {}^C_0 D^\gamma_t E(t) \right|_{E=0} = f(S)(g_1(I_1) + g_2(I_2)) \geq 0,$$
$$\left. {}^C_0 D^\gamma_t I_1(t) \right|_{I_1=0} = p\epsilon E \geq 0,$$
$$\left. {}^C_0 D^\gamma_t I_2(t) \right|_{I_2=0} = q\epsilon E \geq 0,$$
$$\left. {}^C_0 D^\gamma_t R(t) \right|_{R=0} = r_1 I_1 + r_2 I_2 \geq 0.$$

According to the Generalized Mean Value Theorem in reference[36], the solutions are non-negative and remain within $\mathbb{R}^5_+$.

Define $N(t) = S(t) + E(t) + I_1(t) + I_2(t) + R(t)$. From system (3), we obtain

$$\begin{aligned} {}^C_0 D^\gamma_t N(t) &= \Lambda - \mu(S(t) + E(t) + I_1(t) + I_2(t) + R(t)) - \alpha I_1 - \alpha I_2 \\ &\leq \Lambda - \mu N(t). \end{aligned}$$

Therefore, by Lemma 2.2, we obtain the following result,

$$N(t) \leq (N(0) - \frac{\Lambda}{\mu})E_\gamma(-\mu t^\gamma) + \frac{\Lambda}{\mu}.$$

By considering the asymptotic behavior of the Mittag-Leffler function as $t \to \infty$, we finally obtain $N(t) \leq S_0$.

Thus, the region Ω is positively invariant, this is sufficient to analyze the dynamics of system (3) in region Ω. $\square$

Stability analysis

Firstly, we use the the next-generation matrix method[37] to calculate R_0 of system (3), $x = (E, I_1, I_2, S, R)^T, x_0 = (0, 0, 0, S_0, 0)^T$, where $S_0 = \frac{\Lambda}{\mu}, {}^C_0 D^\gamma_t x(t) = \mathscr{F} - \mathscr{V}$, where

$$\mathscr{F} = \begin{pmatrix} f(S)(g_1(I_1) + g_2(I_2)) \\ 0 \\ 0 \\ 0 \\ 0 \end{pmatrix}, \quad \mathscr{V} = \begin{pmatrix} (\epsilon + \mu)E \\ -p\epsilon E + (\mu + \alpha + r_1)I_1 \\ -q\epsilon E + (\mu + \alpha + r_2)I_2 \\ -\Lambda + f(S)(g_1(I_1) + g_2(I_2)) + \mu S \\ -r_1 I_1 - r_2 I_2 + \mu R \end{pmatrix}.$$

Calculate the Jacobian matrix

$$F \mid_{x_0} = \begin{pmatrix} 0 & f(S)g_1'(I_1) & f(S)g_2'(I_2) \\ 0 & 0 & 0 \\ 0 & 0 & 0 \end{pmatrix} \Bigg|_{x_0} = \begin{pmatrix} 0 & f(S_0)g_1'(0) & f(S_0)g_2'(0) \\ 0 & 0 & 0 \\ 0 & 0 & 0 \end{pmatrix}.$$

$$V \mid_{x_0} = \begin{pmatrix} \epsilon + \mu & 0 & 0 \\ -p\epsilon & \mu + \alpha + r_1 & 0 \\ -q\epsilon & 0 & \mu + \alpha + r_2 \end{pmatrix}, \quad V^{-1} = \begin{pmatrix} \frac{1}{\epsilon+\mu} & 0 & 0 \\ \frac{p\epsilon}{(\epsilon+\mu)(\mu+\alpha+r_1)} & \frac{1}{\mu+\alpha+r_1} & 0 \\ \frac{q\epsilon}{(\epsilon+\mu)(\mu+\alpha+r_2)} & 0 & \frac{1}{\mu+\alpha+r_2} \end{pmatrix}.$$

Therefore

$$R_0 = \rho(FV^{-1}) = \frac{f(S_0)g_1'(0)p\epsilon}{(\epsilon+\mu)(\mu+\alpha+r_1)} + \frac{f(S_0)g_2'(0)q\epsilon}{(\epsilon+\mu)(\mu+\alpha+r_2)}.$$

Let the basic reproduction number for symptomatic individuals be $R_1 = \frac{\Lambda \beta_1 p \epsilon}{\mu(\epsilon+\mu)(\mu+\alpha+r_1)}$, and for asymptomatic individuals be $R_2 = \frac{\Lambda \beta_2 q \epsilon}{\mu(\epsilon+\mu)(\mu+\alpha+r_2)}$. Then, the overall basic reproduction number is $R_0 = R_1 + R_2$, which accounts for the transmission contributions from both symptomatic and asymptomatic individuals.

The disease-free equilibrium of System (3) is given by $P_0(S_0, 0, 0, 0, 0)$, where $S_0 = \frac{\Lambda}{\mu}$. We now proceed to establish the existence and uniqueness of the positive equilibrium point, setting

$$\begin{cases} \Lambda - f(S)(g_1(I_1) + g_2(I_2)) - \mu S = 0, \\ f(S)(g_1(I_1) + g_2(I_2)) - (\epsilon + \mu)E = 0, \\ p\epsilon E - (\mu + \alpha + r_1)I_1 = 0, \\ q\epsilon E - (\mu + \alpha + r_2)I_2 = 0, \\ r_1 I_1 + r_2 I_2 - \mu R = 0. \end{cases} \tag{5}$$

By adding the first two equations of (5), we obtain

$$S = \frac{\Lambda}{\mu} - \frac{\epsilon + \mu}{\mu}E. \tag{6}$$

From the third equation of (5), we deduce

$$I_1 = \frac{p\epsilon}{\mu + \alpha + r_1}E. \tag{7}$$

From the firth equation, it follows that

$$I_2 = \frac{q\epsilon}{\mu + \alpha + r_2}E. \tag{8}$$

Substituting them into the second equation of (5), we obtain

$$f\left(\frac{\Lambda}{\mu} - \frac{\epsilon + \mu}{\mu}E\right)\left[g_1\left(\frac{p\epsilon}{\mu + \alpha + r_1}E\right) + g_2\left(\frac{q\epsilon}{\mu + \alpha + r_2}E\right)\right] - (\epsilon + \mu)E = 0.$$

Define

$$\Psi(E) = f\left(\frac{\Lambda}{\mu} - \frac{\epsilon + \mu}{\mu}E\right)\left[g_1\left(\frac{p\epsilon}{\mu + \alpha + r_1}E\right) + g_2\left(\frac{q\epsilon}{\mu + \alpha + r_2}E\right)\right] - (\epsilon + \mu)E.$$

It is known that $\Psi(0) = 0$ and $\Psi\left(\frac{\Lambda}{\epsilon+\mu}\right) = -\Lambda < 0$. Hence, we will study the existence and uniqueness of the positive equilibrium point within the interval $(0, \frac{\Lambda}{\epsilon+\mu})$. Taking the derivative of both sides of the equation, we get

$$\Psi'(E) = -\frac{\epsilon+\mu}{\mu}f'\left(\frac{\Lambda}{\mu}-\frac{\epsilon+\mu}{\mu}E\right)\left[g_1\left(\frac{p\epsilon}{\mu+\alpha+r_1}E\right)+g_2\left(\frac{q\epsilon}{\mu+\alpha+r_2}E\right)\right]$$

$$+f\left(\frac{\Lambda}{\mu}-\frac{\epsilon+\mu}{\mu}E\right)\left[\frac{p\epsilon}{\mu+\alpha+r_1}g_1'\left(\frac{p\epsilon}{\mu+\alpha+r_1}E\right)\right.$$

$$\left.+\frac{q\epsilon}{\mu+\alpha+r_2}g_2'\left(\frac{q\epsilon}{\mu+\alpha+r_2}E\right)\right]-(\epsilon+\mu).$$

$$\Psi'(0) = -\frac{\epsilon+\mu}{\mu}f'\left(\frac{\Lambda}{\mu}\right)\left(g_1(0)+g_2(0)\right)+f\left(\frac{\Lambda}{\mu}\right)\left[\frac{p\epsilon}{\mu+\alpha+r_1}g_1'(0)\right.$$

$$\left.+\frac{q\epsilon}{\mu+\alpha+r_2}g_2'(0)\right]-(\epsilon+\mu)$$

$$= -(\epsilon+\mu)+f\left(\frac{\Lambda}{\mu}\right)\left[\frac{p\epsilon}{\mu+\alpha+r_1}g_1'(0)+\frac{q\epsilon}{\mu+\alpha+r_2}g_2'(0)\right]$$

$$= (\epsilon+\mu)\left[\frac{f\left(\frac{\Lambda}{\mu}\right)p\epsilon}{(\epsilon+\mu)(\mu+\alpha+r_1)}g_1'(0)+\frac{f\left(\frac{\Lambda}{\mu}\right)q\epsilon}{(\epsilon+\mu)(\mu+\alpha+r_2)}g_2'(0)-1\right]$$

$$= (\epsilon+\mu)(R_0-1).$$

When $R_0 > 1$, it follows that $\Psi'(0) > 0$. Let $P^*(S^*, E^*, I_1^*, I_2^*, R^*)$ represent an equilibrium point within the interval $(0, \frac{\Lambda}{\epsilon+\mu})$. These variables satisfy equations (6), (7), and (8). Thus, we have

$$\Psi'(E^*) = -\frac{\epsilon+\mu}{\mu}f'\left(\frac{\Lambda}{\mu}-\frac{\epsilon+\mu}{\mu}E^*\right)\left[g_1\left(\frac{p\epsilon}{\mu+\alpha+r_1}E^*\right)+g_2\left(\frac{q\epsilon}{\mu+\alpha+r_2}E^*\right)\right]$$

$$+f\left(\frac{\Lambda}{\mu}-\frac{\epsilon+\mu}{\mu}E^*\right)\left[\frac{p\epsilon}{\mu+\alpha+r_1}g_1'\left(\frac{p\epsilon}{\mu+\alpha+r_1}E^*\right)\right.$$

$$\left.+\frac{q\epsilon}{\mu+\alpha+r_2}g_2'\left(\frac{q\epsilon}{\mu+\alpha+r_2}E^*\right)\right]-(\epsilon+\mu)$$

$$= -\frac{\epsilon+\mu}{\mu}f'(S^*)\left(g_1(I_1^*)+g_2(I_2^*)\right)+f(S^*)\left[\frac{p\epsilon}{\mu+\alpha+r_1}g_1'(I_1^*)\right.$$

$$\left.+\frac{q\epsilon}{\mu+\alpha+r_2}g_2'(I_2^*)\right]-(\epsilon+\mu).$$

Under the condition that $\frac{g_1(I_1)}{I_1}$ and $\frac{g_2(I_2)}{I_2}$ are non-increasing, it follows that for $I_1 > 0$ and $I_2 > 0$, we have $g_1'(I_1) \le \frac{g_1(I_1)}{I_1}$ and $g_2'(I_2) \le \frac{g_2(I_2)}{I_2}$, then

$$\Psi'(E^*) \le -(\epsilon+\mu)-\frac{\epsilon+\mu}{\mu}f'(S^*)(g_1(I_1^*)+g_2(I_2^*))$$

$$+f(S^*)\left(\frac{p\epsilon}{\mu+\alpha+r_1}\frac{g_1(I_1^*)}{I_1^*}+\frac{q\epsilon}{\mu+\alpha+r_2}\frac{g_2(I_2^*)}{I_2^*}\right)$$

$$= -(\epsilon+\mu)-\frac{\epsilon+\mu}{\mu}f'(S^*)(g_1(I_1^*)+g_2(I_2^*))+\frac{f(S^*)}{E^*}(g_1(I_1^*)+g_2(I_2^*))$$

$$= -\frac{\epsilon+\mu}{\mu}f'(S^*)(g_1(I_1^*)+g_2(I_2^*))$$

$$< 0.$$

Thus, when the basic reproduction number $R_0 > 1$, there exists a unique positive equilibrium point.

Theorem 4.1 When $R_0 < 1$, then the P_0 is global asymptotic stability.

Proof Define the Lyapunov function as follows

$$V_1(t) = C_1 \int_{S_0}^{S(t)} \frac{f(\tau)-f(S_0)}{f(\tau)}d\tau + C_2 E + C_3 I_1 + C_4 I_2,$$

where C_1, C_2, C_3, C_4 are positive constant. By Lemma 2.3, it can be concluded that

$$
\begin{aligned}
{}_0^C D_t^\gamma V_1(t) &\leq C_1\left(1 - \frac{f(S_0)}{f(S)}\right){}_0^C D_t^\gamma S(t) + C_2\,{}_0^C D_t^\gamma E(t) + C_3\,{}_0^C D_t^\gamma I_1(t) + C_4\,{}_0^C D_t^\gamma I_2(t) \\
&= C_1\left(1 - \frac{f(S_0)}{f(S)}\right)(\Lambda - f(S)(g_1(I_1) + g_2(I_2)) - \mu S - (\Lambda - \mu S_0)) \\
&\quad + C_2\left(f(S)(g_1(I_1) + g_2(I_2)) - (\epsilon + \mu)E\right) \\
&\quad + C_3\left(p\epsilon E - (\mu + \alpha + r_1)I_1\right) + C_4\left(q\epsilon E - (\mu + \alpha + r_2)I_2\right) \\
&= C_1\left(1 - \frac{f(S_0)}{f(S)}\right)(-\mu(S - S_0) - f(S)(g_1(I_1) + g_2(I_2))) \\
&\quad + C_2 f(S)(g_1(I_1) + g_2(I_2)) - C_2(\epsilon + \mu)E \\
&\quad + C_3 p\epsilon E - C_3(\mu + \alpha + r_1)I_1 + C_4 q\epsilon E - C_4(\mu + \alpha + r_2)I_2 \\
&= C_1(-\mu(S - S_0))\left(1 - \frac{f(S_0)}{f(S)}\right) - C_1 f(S)(g_1(I_1) + g_2(I_2)) \\
&\quad + C_1 f(S_0)(g_1(I_1) + g_2(I_2)) + C_2 f(S)(g_1(I_1) + g_2(I_2)) - C_2(\epsilon + \mu)E \\
&\quad + C_3 p\epsilon E - C_3(\mu + \alpha + r_1)I_1 + C_4 q\epsilon E - C_4(\mu + \alpha + r_2)I_2,
\end{aligned}
$$

Let $C_1 = C_2 = 1$, we have

$$
\begin{aligned}
{}_0^C D_t^\gamma V_1(t) &\leq -\mu(S - S_0)\left(1 - \frac{f(S_0)}{f(S)}\right) + f(S_0)(g_1(I_1) + g_2(I_2)) - (\epsilon + \mu)E \\
&\quad + C_3 p\epsilon E - C_3(\mu + \alpha + r_1)I_1 + C_4 q\epsilon E - C_4(\mu + \alpha + r_2)I_2 \\
&= -\mu(S - S_0)\left(1 - \frac{f(S_0)}{f(S)}\right) - (\epsilon + \mu)E + C_3 p\epsilon E + C_4 q\epsilon E \\
&\quad + (f(S_0)g_1(I_1) - C_3(\mu + \alpha + r_1)I_1) + (f(S_0)g_2(I_2) - C_4(\mu + \alpha + r_2)I_2).
\end{aligned}
$$

If $C_3 \geq \frac{f(S_0)}{(\mu + \alpha + r_1)}\frac{g_1(I_1)}{I_1}$ and $C_4 \geq \frac{f(S_0)}{(\mu + \alpha + r_2)}\frac{g_2(I_2)}{I_2}$, then

$$
f(S_0)g_1(I_1) - C_3(\mu + \alpha + r_1)I_1 \leq 0, \quad f(S_0)g_2(I_2) - C_4(\mu + \alpha + r_2)I_2 \leq 0.
$$

Under the condition that $\frac{g_1(I_1)}{I_1}$ and $\frac{g_2(I_2)}{I_2}$ are non-increasing, it follows that

$$
\frac{g_1(I_1)}{I_1} \leq \lim_{x \to 0^+} \frac{g_1(I_1)}{I_1}, \quad \frac{g_2(I_2)}{I_2} \leq \lim_{x \to 0^+} \frac{g_2(I_2)}{I_2}.
$$

To determine a specific value for C_3 and C_4, we can consider the limit as I_1, I_2 approaches 0^+. Taking the limit, we have

$$
\lim_{I_1 \to 0^+} \frac{g_1(I_1)}{I_1} = \lim_{I_1 \to 0^+} \frac{g_1(I_1) - g_1(0)}{I_1 - 0} = g_1{}'(0), \quad \lim_{I_2 \to 0^+} \frac{g_2(I_2)}{I_2} = \lim_{I_2 \to 0^+} \frac{g_2(I_2) - g_2(0)}{I_2 - 0} = g_2{}'(0),
$$

then let

$$
C_3 = \frac{f(S_0)}{\mu + \alpha + r_1}g_1{}'(0), \quad C_4 = \frac{f(S_0)}{\mu + \alpha + r_2}g_2{}'(0),
$$

then

$$
\begin{aligned}
{}_0^C D_t^\gamma V_1(t) &\leq -\mu(S - S_0)\left(1 - \frac{f(S_0)}{f(S)}\right) - (\epsilon + \mu)E + \frac{f(S_0)g_1{}'(0)}{\mu + \alpha + r_1}p\epsilon E + \frac{f(S_0)g_2{}'(0)}{\mu + \alpha + r_2}q\epsilon E \\
&= -\mu(S - S_0)\left(1 - \frac{f(S_0)}{f(S)}\right) + (\epsilon + \mu)\left(\frac{f(S_0)g_1{}'(0)}{(\epsilon + \mu)(\mu + \alpha + r_1)}p\epsilon \right. \\
&\quad + \left.\frac{f(S_0)g_2{}'(0)}{(\epsilon + \mu)(\mu + \alpha + r_2)}q\epsilon - 1\right)E \\
&= -\mu(S - S_0)\left(1 - \frac{f(S_0)}{f(S)}\right) + (\epsilon + \mu)(R_0 - 1)E.
\end{aligned}
$$

According to the mean value theorem, it follows that $-\mu(S - S_0)\left(1 - \frac{f(S_0)}{f(S)}\right) \leq 0$, thus, if $R_0 \leq 1$, then ${}_0^C D_t^\gamma V_1(t) \leq 0$.

Moreover, $_0^C D_t^\gamma V_1(t) = 0$ if and only if $P = P_0$. Therefore, according to LaSalle's invariance principle, when $R_0 < 1$, the disease-free equilibrium point P_0 is globally asymptotically stable in the interior of Ω. $\square$

Theorem 4.2 When $R_0 > 1$, then the P^* is global asymptotic stability.

Proof Let the Lyapunov function be defined as follows

$$V_2(t) = C_1 \int_{S^*}^{S} \frac{f(\tau) - f(S^*)}{f(\tau)} d\tau + C_2 \int_{E^*}^{E} \frac{\tau - E^*}{\tau} d\tau + C_3 \int_{I_1^*}^{I_1} \frac{\tau - I_1^*}{\tau} d\tau + C_4 \int_{I_2^*}^{I_2} \frac{\tau - I_2^*}{\tau} d\tau,$$

where C_1, C_2, C_3, C_4 are positive constant. By Lemma 2.3, it follows that

$$\begin{aligned}
_0^C D_t^\gamma V_2(t) \leq{} & C_1 \left(1 - \frac{f(S^*)}{f(S)}\right) {}_0^C D_t^\gamma S(t) + C_2 \left(1 - \frac{E^*}{E}\right) {}_0^C D_t^\gamma E(t) \\
& + C_3 \left(1 - \frac{I_1^*}{I_1}\right) {}_0^C D_t^\gamma I_1(t) + C_4 \left(1 - \frac{I_2^*}{I_2}\right) {}_0^C D_t^\gamma I_2(t).
\end{aligned}$$

Thus, we can get

$$\begin{aligned}
_0^C D_t^\gamma V_2(t) \leq{} & C_1 \left(1 - \frac{f(S^*)}{f(S)}\right) [\Lambda - f(S)(g_1(I_1) + g_2(I_2)) - \mu S \\
& - (\Lambda - f(S^*)(g_1(I_1^*) + g_2(I_2^*)) - \mu S^*)] \\
& + C_2 \left(1 - \frac{E^*}{E}\right) [f(S)(g_1(I_1) + g_2(I_2)) - (\epsilon + \mu)E \\
& - (f(S^*)(g_1(I_1^*) + g_2(I_2^*)) - (\epsilon + \mu)E^*)] \\
& + C_3 \left(1 - \frac{I_1^*}{I_1}\right) [p\epsilon E - (\mu + \alpha + r_1)I_1 - (p\epsilon E^* - (\mu + \alpha + r_1)I_1^*)] \\
& + C_4 \left(1 - \frac{I_2^*}{I_2}\right) [q\epsilon E - (\mu + \alpha + r_2)I_2 - (q\epsilon E^* - (\mu + \alpha + r_2)I_2^*)] \\
={} & C_1 \left(1 - \frac{f(S^*)}{f(S)}\right) [-\mu(S - S^*) - (f(S)g_1(I_1) - f(S^*)g_1(I_1^*)) \\
& - (f(S)g_2(I_2) - f(S^*)g_2(I_2^*))] \\
& + C_2 \left(1 - \frac{E^*}{E}\right) [(f(S)g_1(I_1) - f(S^*)g_1(I_1^*)) + (f(S)g_2(I_2) - f(S^*)g_2(I_2^*)) \\
& - (\epsilon + \mu)(E - E^*)] \\
& + C_3 \left(1 - \frac{I_1^*}{I_1}\right) [p\epsilon(E - E^*) - (\mu + \alpha + r_1)(I_1 - I_1^*)] \\
& + C_4 \left(1 - \frac{I_2^*}{I_2}\right) [q\epsilon(E - E^*) - (\mu + \alpha + r_2)(I_2 - I_2^*)] \\
={} & C_1 \left(1 - \frac{f(S^*)}{f(S)}\right) \left[-\mu(S - S^*) - f(S^*)g_1(I_1^*) \left(\frac{f(S)g_1(I_1)}{f(S^*)g_1(I_1^*)} - 1\right) \right. \\
& \left. - f(S^*)g_2(I_2^*) \left(\frac{f(S)g_2(I_2)}{f(S^*)g_2(I_2^*)} - 1\right)\right] \\
& + C_2 \left(1 - \frac{E^*}{E}\right) \left[f(S^*)g_1(I_1^*) \left(\frac{f(S)g_1(I_1)}{f(S^*)g_1(I_1^*)} - 1\right) \right. \\
& \left. + f(S^*)g_2(I_2^*) \left(\frac{f(S)g_2(I_2)}{f(S^*)g_2(I_2^*)} - 1\right)\right] \\
& - C_2 \left(1 - \frac{E^*}{E}\right) (\epsilon + \mu)E^* \left(\frac{E}{E^*} - 1\right) \\
& + C_3 \left(1 - \frac{I_1^*}{I_1}\right) \left[p\epsilon E^* \left(\frac{E}{E^*} - 1\right) - (\mu + \alpha + r_1)I_1^* \left(\frac{I_1}{I_1^*} - 1\right)\right] \\
& + C_4 \left(1 - \frac{I_2^*}{I_2}\right) \left[q\epsilon E^* \left(\frac{E}{E^*} - 1\right) - (\mu + \alpha + r_2)I_2^* \left(\frac{I_2}{I_2^*} - 1\right)\right].
\end{aligned}$$

Due to $p\epsilon E^* = (\mu + \alpha + r_1)I_1^*$ and $q\epsilon E^* = (\mu + \alpha + r_2)I_2^*$, we can get

$$
{}^{C}_{0}D^{\gamma}_{t}V_2(t) \leq C_1\left[-\mu(S-S^*)\left(1-\frac{f(S^*)}{f(S)}\right)\right]
$$

$$
-C_1 f(S^*)g_1(I_1^*)\left(\frac{f(S)g_1(I_1)}{f(S^*)g_1(I_1^*)}-1\right)\left(1-\frac{f(S^*)}{f(S)}\right)
$$

$$
-C_1 f(S^*)g_2(I_2^*)\left(\frac{f(S)g_2(I_2)}{f(S^*)g_2(I_2^*)}-1\right)\left(1-\frac{f(S^*)}{f(S)}\right)
$$

$$
+C_2 f(S^*)g_1(I_1^*)\left(\frac{f(S)g_1(I_1)}{f(S^*)g_1(I_1^*)}-1\right)\left(1-\frac{E^*}{E}\right)
$$

$$
+C_2 f(S^*)g_2(I_2^*)\left(\frac{f(S)g_2(I_2)}{f(S^*)g_2(I_2^*)}-1\right)\left(1-\frac{E^*}{E}\right)
$$

$$
-C_2(\epsilon+\mu)E^*\left(1-\frac{E^*}{E}\right)\left(\frac{E}{E^*}-1\right)
$$

$$
+C_3 p\epsilon E^*\left(\frac{E}{E^*}-1\right)\left(1-\frac{I_1^*}{I_1}\right)-C_3(\mu+\alpha+r_1)I_1^*\left(\frac{I_1}{I_1^*}-1\right)\left(1-\frac{I_1^*}{I_1}\right)
$$

$$
+C_4 q\epsilon E^*\left(\frac{E}{E^*}-1\right)\left(1-\frac{I_2^*}{I_2}\right)-C_4(\mu+\alpha+r_2)I_2^*\left(\frac{I_2}{I_2^*}-1\right)\left(1-\frac{I_2^*}{I_2}\right)
$$

$$
= C_1\left[-\mu(S-S^*)\left(1-\frac{f(S^*)}{f(S)}\right)\right]
$$

$$
-C_1 f(S^*)g_1(I_1^*)\left(\frac{f(S)g_1(I_1)}{f(S^*)g_1(I_1^*)}-\frac{g_1(I_1)}{g_1(I_1^*)}-1+\frac{f(S^*)}{f(S)}\right)
$$

$$
-C_1 f(S^*)g_2(I_2^*)\left(\frac{f(S)g_2(I_2)}{f(S^*)g_2(I_2^*)}-\frac{g_2(I_2)}{g_2(I_2^*)}-1+\frac{f(S^*)}{f(S)}\right)
$$

$$
+C_2 f(S^*)g_1(I_1^*)\left(\frac{f(S)g_1(I_1)}{f(S^*)g_1(I_1^*)}-\frac{f(S)g_1(I_1)E^*}{f(S^*)g_1(I_1^*)E}-1+\frac{E^*}{E}\right)
$$

$$
+C_2 f(S^*)g_2(I_2^*)\left(\frac{f(S)g_2(I_2)}{f(S^*)g_2(I_2^*)}-\frac{f(S)g_2(I_2)E^*}{f(S^*)g_2(I_2^*)E}-1+\frac{E^*}{E}\right)
$$

$$
-C_2(\epsilon+\mu)E^*\left(\frac{E}{E^*}-2+\frac{E^*}{E}\right)
$$

$$
+C_3 p\epsilon E^*\left(\frac{E}{E^*}-\frac{EI_1^*}{E^*I_1}-1+\frac{I_1^*}{I_1}-\frac{I_1}{I_1^*}+2-\frac{I_1^*}{I_1}\right)
$$

$$
+C_4 q\epsilon E^*\left(\frac{E}{E^*}-\frac{EI_2^*}{E^*I_2}-1+\frac{I_2^*}{I_2}-\frac{I_2}{I_2^*}+2-\frac{I_2^*}{I_2}\right).
$$

We choose $C_1 = C_2 = 1$, as $f(S^*)(g_1(I_1^*) + g_2(I_2^*)) = (\epsilon+\mu)E^*$, then

$$
{}^{C}_{0}D^{\gamma}_{t}V_2(t) \leq -\mu(S-S^*)\left(1-\frac{f(S^*)}{f(S)}\right)
$$

$$
-f(S^*)g_1(I_1^*)\left(\frac{f(S)g_1(I_1)}{f(S^*)g_1(I_1^*)}-\frac{g_1(I_1)}{g_1(I_1^*)}-1+\frac{f(S^*)}{f(S)}\right.
$$

$$
\left.-\frac{f(S)g_1(I_1)}{f(S^*)g_1(I_1^*)}+\frac{f(S)g_1(I_1)E^*}{f(S^*)g_1(I_1^*)E}+1-\frac{E^*}{E}+\frac{E}{E^*}-2+\frac{E^*}{E}\right)
$$

$$
-f(S^*)g_2(I_2^*)\left(\frac{f(S)g_2(I_2)}{f(S^*)g_2(I_2^*)}-\frac{g_2(I_2)}{g_2(I_2^*)}-1+\frac{f(S^*)}{f(S)}\right.
$$

$$
\left.-\frac{f(S)g_2(I_2)}{f(S^*)g_2(I_2^*)}+\frac{f(S)g_2(I_2)E^*}{f(S^*)g_2(I_2^*)E}+1-\frac{E^*}{E}+\frac{E}{E^*}-2+\frac{E^*}{E}\right)
$$

$$
+C_3 p\epsilon E^*\left(\frac{E}{E^*}-\frac{EI_1^*}{E^*I_1}+1-\frac{I_1}{I_1^*}\right)
$$

$$
+C_4 q\epsilon E^*\left(\frac{E}{E^*}-\frac{EI_2^*}{E^*I_2}+1-\frac{I_2}{I_2^*}\right).
$$

10

Let $C_3 = \frac{f(S^*)g_1(I_1^*)}{p\epsilon E^*}, C_4 = \frac{f(S^*)g_2(I_2^*)}{q\epsilon E^*}$, we have

$$
{}_0^C D_t^\gamma V_2(t) \leq -\mu(S - S^*)\left(1 - \frac{f(S^*)}{f(S)}\right)
$$

$$
- f(S^*)g_1(I_1^*)\left(-\frac{g_1(I_1)}{g_1(I_1^*)} + \frac{I_1}{I_1^*} + \frac{f(S^*)}{f(S)} + \frac{f(S)g_1(I_1)E^*}{f(S^*)g_1(I_1^*)E} + \frac{EI_1^*}{E^*I_1} - 3\right)
$$

$$
- f(S^*)g_2(I_2^*)\left(-\frac{g_2(I_2)}{g_2(I_2^*)} + \frac{I_2}{I_2^*} + \frac{f(S^*)}{f(S)} + \frac{f(S)g_2(I_2)E^*}{f(S^*)g_2(I_2^*)E} + \frac{EI_2^*}{E^*I_2} - 3\right).
$$

Let

$$
L_1 = -f(S^*)g_1(I_1^*)\left(-\frac{g_1(I_1)}{g_1(I_1^*)} + \frac{I_1}{I_1^*} + \frac{f(S^*)}{f(S)} + \frac{f(S)g_1(I_1)E^*}{f(S^*)g_1(I_1^*)E} + \frac{EI_1^*}{E^*I_1} - 3\right),
$$

$$
L_2 = -f(S^*)g_2(I_2^*)\left(-\frac{g_2(I_2)}{g_2(I_2^*)} + \frac{I_2}{I_2^*} + \frac{f(S^*)}{f(S)} + \frac{f(S)g_2(I_2)E^*}{f(S^*)g_2(I_2^*)E} + \frac{EI_2^*}{E^*I_2} - 3\right).
$$

Considering $H(x) = x - 1 - \ln x$, then

$$
L_1 = -f(S^*)g_1(I_1^*)\left[-H\left(\frac{g_1(I_1)}{g_1(I_1^*)}\right) + H\left(\frac{I_1}{I_1^*}\right) + H\left(\frac{f(S^*)}{f(S)}\right)\right.
$$

$$
\left. + H\left(\frac{f(S)g_1(I_1)E^*}{f(S^*)g_1(I_1^*)E}\right) + H\left(\frac{EI_1^*}{E^*I_1}\right)\right].
$$

Let

$$
F(I_1) = H\left(\frac{g_1(I_1)}{g_1(I_1^*)}\right) - H\left(\frac{I_1}{I_1^*}\right).
$$

If $F(I_1) \leq 0$, then $L_1 \leq 0$, thus we need to prove that $F(I_1) \leq 0$,

$$
F'(I_1) = \left(1 - \frac{g_1(I_1^*)}{g_1(I_1)}\right)\frac{g_1'(I_1)}{g_1(I_1^*)} - \left(1 - \frac{I_1^*}{I_1}\right)\frac{1}{I_1^*}
$$

$$
= \frac{g_1(I_1) - g_1(I_1^*)}{g_1(I_1)g_1(I_1^*)}g_1'(I_1) - \frac{I_1 - I_1^*}{I_1 I_1^*}.
$$

Since $G_1(I_1) = \frac{g(I_1)}{I_1}$ is non-increasing, we can get when $I_1 > 0$, $g_1'(I_1) \leq \frac{g(I_1)}{I_1}$, then

$$
F'(I_1) \leq \frac{1}{I_1}\left(\frac{g_1(I_1)}{g_1(I_1^*)} - \frac{I_1}{I_1^*}\right).
$$

In case 1, when $I_1 \geq I_1^*$, we have $\frac{g_1(I_1)}{I_1} \leq \frac{g_1(I_1^*)}{I_1^*}$, which implies $\frac{g_1(I_1)}{g_1(I_1^*)} \leq \frac{I_1}{I_1^*}$, Therefore, $F'(I) \leq 0$, for

$F(I^*) = 0$, it follows that $F(I_1) \leq 0$.

In case 2, when $I_1 \leq I_1^*$, we have $\frac{g_1(I_1)}{I_1} \geq \frac{g_1(I_1^*)}{I_1^*}$, which leads to $\frac{g_1(I_1)}{g_1(I_1^*)} \geq \frac{I_1}{I_1^*}$, thus $F'(I_1) \geq 0$ and since

$F(I_1^*) = 0$, we can conclude that $F(I_1) \leq 0$.

In conclusion, for all values of I_1, we have $F(I_1) \leq 0$, which leads to $L_1 \leq 0$. By applying a similar argument, we can also deduce that $L_2 \leq 0$. Also, by the mean value theorem, we can deduce that $-\mu(S - S^*)\left(1 - \frac{f(S^*)}{f(S)}\right) \leq 0$. Thus, we can conclude that

$$
{}_0^C D_t^\gamma V_2(t) = -\mu(S - S^*)\left(1 - \frac{f(S^*)}{f(S)}\right) + L_1 + L_2 \leq 0.
$$

Therefore, if $R_0 > 1$, then ${}_0^C D_t^\gamma V_2(t) \leq 0$, and ${}_0^C D_t^\gamma V_2(t) = 0$ if and only if $P = P^*$, according to LaSalle's invariance principle, this implies that the positive equilibrium point P^* is asymptotically stable within the interior of Ω.□

Sensitivity analysis

To verify the correctness of the theoretical results, we selected a commonly incidence rate function for sensitivity analysis and numerical simulation, we consider $f(S) = S$, $g_1(I) = \beta_1 I_1$ and $g_2(I) = \beta_2 I_2$, we have

$$\begin{cases} {}^C_0 D^\gamma_t S(t) = \Lambda - S(\beta_1 I_1 + \beta_2 I_2) - \mu S, \\ {}^C_0 D^\gamma_t E(t) = S(\beta_1 I_1 + \beta_2 I_2) - (\epsilon + \mu)E, \\ {}^C_0 D_t I_1(t) = p\epsilon E - (\mu + \alpha + r_1)I_1, \\ {}^C_0 D_t I_2(t) = q\epsilon E - (\mu + \alpha + r_2)I_2, \\ {}^C_0 D^\gamma_t R(t) = r_1 I_1 + r^\gamma_2 I_2 - \mu R. \end{cases} \tag{9}$$

System (9) always has a disease-free equilibrium $P_0(S_0, 0, 0, 0, 0)$, where $S_0 = \frac{\Lambda}{\mu}$, the basic reproduction number for system (9) is

$$R_0 = \frac{\Lambda \beta_1 p \epsilon}{\mu(\epsilon + \mu)(\mu + \alpha + r_1)} + \frac{\Lambda \beta_2 q \epsilon}{\mu(\epsilon + \mu)(\mu + \alpha + r_2)},$$

and $R_1 = \frac{\Lambda \beta_1 p \epsilon}{\mu(\epsilon+\mu)(\mu+\alpha+r_1)}$, $R_2 = \frac{\Lambda \beta_2 q \epsilon}{\mu(\epsilon+\mu)(\mu+\alpha+r_2)}$, $R_0 = R_1 + R_2$.

We calculate the partial derivatives of the R_0 with respect to the relevant parameters as follows,

$$\begin{aligned} \frac{\partial R_0}{\partial \alpha} &= -\left(\frac{R_1}{\mu + \alpha + r_1} + \frac{R_2}{\mu + \alpha + r_2}\right), \\ \frac{\partial R_0}{\partial r_1} &= -\frac{R_1}{\mu + \alpha + r_1}, \quad \frac{\partial R_0}{\partial r_2} = -\frac{R_2}{\mu + \alpha + r_2}, \\ \frac{\partial R_0}{\partial \Lambda} &= \frac{\beta_1 p \epsilon}{\mu(\epsilon + \mu)(\mu + \alpha + r_1)} + \frac{\beta_2 q \epsilon}{\mu(\epsilon + \mu)(\mu + \alpha + r_2)}, \\ \frac{\partial R_0}{\partial \beta_1} &= \frac{\Lambda p \epsilon}{\mu(\epsilon + \mu)(\mu + \alpha + r_1)}, \quad \frac{\partial R_0}{\partial \beta_2} = \frac{\Lambda q \epsilon}{\mu(\epsilon + \mu)(\mu + \alpha + r_2)}, \\ \frac{\partial R_0}{\partial p} &= \frac{\Lambda \beta_1 \epsilon}{\mu(\epsilon + \mu)(\mu + \alpha + r_1)}, \quad \frac{\partial R_0}{\partial q} = \frac{\Lambda \beta_2 \epsilon}{\mu(\epsilon + \mu)(\mu + \alpha + r_2)}, \\ \frac{\partial R_0}{\partial \epsilon} &= \frac{\mu}{\epsilon + \mu} \frac{\Lambda \beta_1 p}{\mu(\epsilon + \mu)(\mu + \alpha + r_1)} + \frac{\mu}{\epsilon + \mu} \frac{\Lambda \beta_2 q}{\mu(\epsilon + \mu)(\mu + \alpha + r_2)}, \\ \frac{\partial R_0}{\partial \mu} &= -\left(\frac{R_1}{\mu} + \frac{R_1}{\epsilon + \mu} + \frac{R_1}{\mu + \alpha + r_1} + \frac{R_2}{\mu} + \frac{R_2}{\epsilon + \mu} + \frac{R_2}{\mu + \alpha + r_2}\right). \end{aligned}$$

It can be observed that the partial derivatives of the basic reproduction number with respect to parameters Λ, β_1, β_2, p, q, and ϵ are positive, indicating that the basic reproduction number increases as these parameters increase. On the other hand, the partial derivatives with respect to parameters μ, α, r_1, and r_2 are negative, indicating that the basic reproduction number decreases as these parameters decrease.
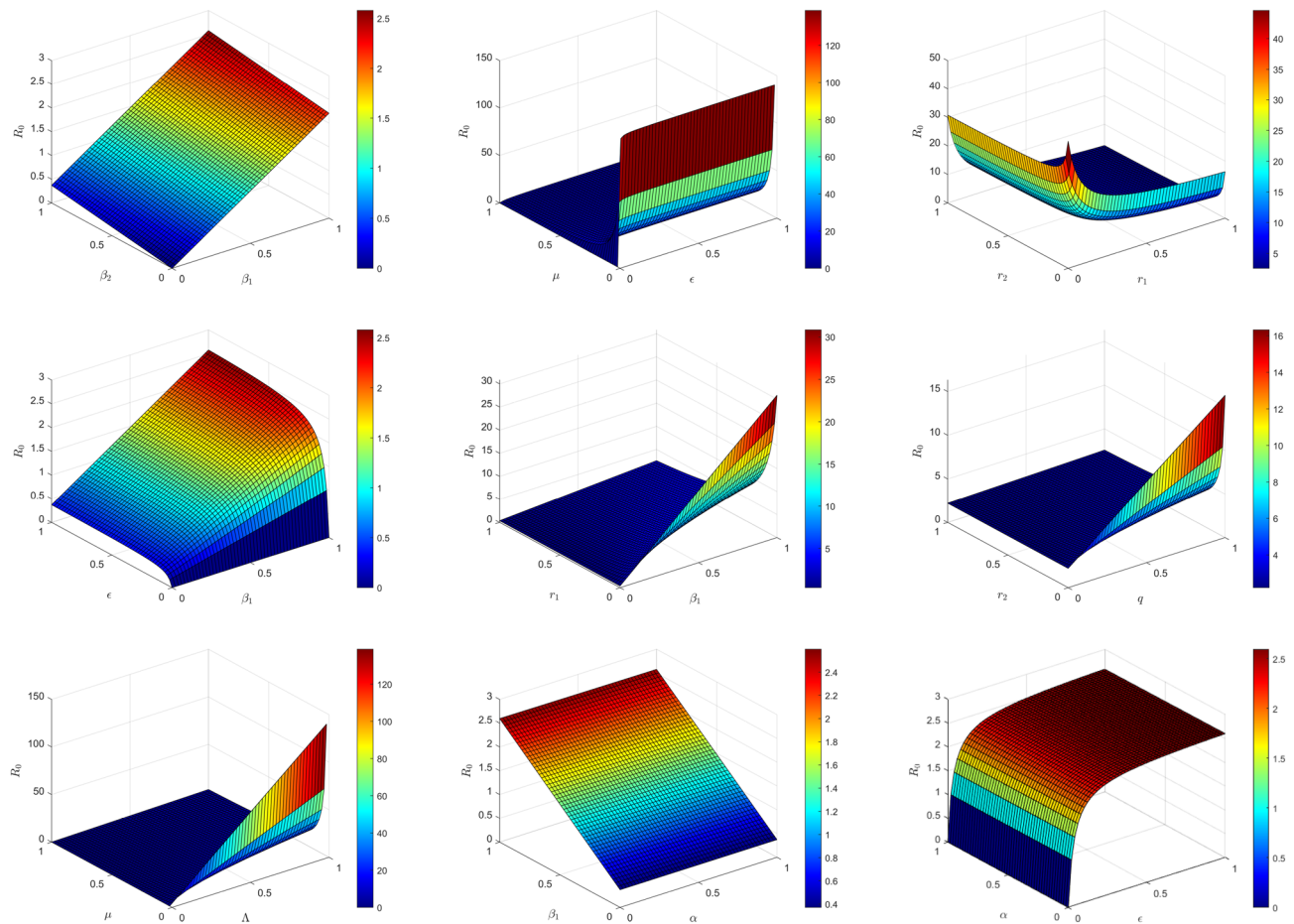
According to reference[38], the normalized forward sensitivity index of a parameter ρ is defined as

$$\varphi^{R_0}_\rho = \frac{\partial R_0}{\partial \rho} \frac{\rho}{|R_0|}.$$

Therefore, the influence of these parameters on R_0 is given by the sensitivity indices as follows

$$\begin{aligned} \varphi^{R_0}_\alpha &= \frac{\partial R_0}{\partial \alpha} \cdot \frac{\alpha}{R_0} = -\left(\frac{\alpha}{\mu + \alpha + r_1} \cdot \frac{R_1}{R_0} + \frac{\alpha}{\mu + \alpha + r_2} \cdot \frac{R_2}{R_0}\right), \\ \varphi^{R_0}_\Lambda &= \frac{\partial R_0}{\partial \Lambda} \cdot \frac{\Lambda}{R_0} = 1, \quad \varphi^{R_0}_{\beta_1} = \frac{\partial R_0}{\partial \beta_1} \cdot \frac{\beta_1}{R_0} = \frac{R_1}{R_0}, \quad \varphi^{R_0}_{\beta_2} = \frac{\partial R_0}{\partial \beta_2} \cdot \frac{\beta_2}{R_0} = \frac{R_2}{R_0}, \\ \varphi^{R_0}_{r_1} &= \frac{\partial R_0}{\partial r_1} \cdot \frac{r_1}{R_0} = -\frac{r_1}{\mu + \alpha + r_1} \cdot \frac{R_1}{R_0}, \quad \varphi^{R_0}_{r_2} = \frac{\partial R_0}{\partial r_2} \cdot \frac{r_2}{R_0} = -\frac{r_2}{\mu + \alpha + r_2} \cdot \frac{R_2}{R_0}, \\ \varphi^{R_0}_\mu &= \frac{\partial R_0}{\partial \mu} \cdot \frac{\mu}{R_0} = -\left(\frac{\mu}{\epsilon + \mu} + 1 + \frac{\mu}{\mu + \alpha + r_1}\right) \frac{R_1}{R_0} - \left(\frac{\mu}{\epsilon + \mu} + 1 + \frac{\mu}{\mu + \alpha + r_2}\right) \frac{R_2}{R_0}, \\ \varphi^{R_0}_p &= \frac{\partial R_0}{\partial p} \cdot \frac{p}{R_0} = \frac{R_1}{R_0}, \quad \varphi^{R_0}_q = \frac{\partial R_0}{\partial q} \cdot \frac{q}{R_0} = \frac{R_2}{R_0}, \quad \varphi^{R_0}_\epsilon = \frac{\partial R_0}{\partial \epsilon} \cdot \frac{\epsilon}{R_0} = \frac{\mu}{\epsilon + \mu}. \end{aligned}$$

Figure 2, it can be observed that the basic reproduction number R_0 has a significant positive correlation with the incidence rate parameters β_1 and β_2, indicating that a higher incidence rate is crucial for disease transmission. Furthermore, the rate of diagnosed individuals ϵ showed a positive correlation with R_0, while the recovery rates r_1 and r_2 exhibited a negative correlation with R_0, suggesting that accelerating recovery rates is a essential

Fig. 2. Effect of sensitive parameters.

for controlling disease spread. The Λ had a positive impact on R_0, whereas the natural mortality rate μ had a negative impact on R_0. Moreover, a higher disease-related mortality rate α significantly reduced R_0, indicting that while deadly diseases are dangerous, their spread may be inherently limited. Overall, the trends in the figure are highly consistent with sensitivity analysis results, emphasizing the importance of targeted interventions focusing on the incidence rate, recovery rate, and latent period for controlling disease transmission.

In summary, the transmission rates β_1, β_2, and the latent period conversion rate ϵ are the most influential parameters for R_0, determining the speed and severity of disease spread. Recovery rates r_1 and r_2 have a secondary influence, but they can be improved through medical interventions. The natural death rate μ and disease mortality rate α have less impact and are not the main intervention targets. The model's stability is highly sensitive to β and ϵ, indicating that small changes in these parameters can significantly alter the disease transmission pattern. Therefore, public health policies should prioritize controlling and improving recovery rates to lower R_0 and stabilize the epidemic.

Numerical simulations

Simulations used MATLAB R2023a on an Intel i7-11800H, with 2× longer runtime for fractional cases.

In order to keep the dimensions of the model the same, we have

$$
\begin{cases}
{}_0^C D_t^\gamma S(t) = \Lambda^\gamma - S(\beta_1^\gamma I_1 + \beta_2^\gamma I_2) - \mu^\gamma S, \\
{}_0^C D_t^\gamma E(t) = S(\beta_1^\gamma I_1 + \beta_2^\gamma I_2) - (\epsilon^\gamma + \mu^\gamma)E, \\
{}_0^C D_t^\gamma I_1(t) = p\epsilon^\gamma E - (\mu^\gamma + \alpha^\gamma + r_1^\gamma)I_1, \\
{}_0^C D_t^\gamma I_2(t) = q\epsilon^\gamma E - (\mu^\gamma + \alpha^\gamma + r_2^\gamma)I_2, \\
{}_0^C D_t^\gamma R(t) = r_1^\gamma I_1 + r_2^\gamma I_2 - \mu^\gamma R.
\end{cases}
\tag{10}
$$

System (10) consistently admits a disease-free equilibrium, denoted as $P_0(S_0, 0, 0, 0, 0)$, where $S_0 = \frac{\Lambda^\gamma}{\mu^\gamma}$. The basic reproduction number corresponding to system (10) is given as follows

Parameters	The first set of values	The second set of values	References
β_1	2.65×10^{-8}	2.65×10^{-11}	[14,39]
β_2	2.65×10^{-8}	2.65×10^{-11}	[14,39]
Λ	100,000	100,000	[14]
μ	7.14×10^{-3}	7.14×10^{-3}	[40]
ϵ	0.2	0.2	[39]
p	0.6834	0.6834	[39]
q	0.3166	0.3166	[39]
α	0.0009	0.0009	[39]
r_1	0.1029	0.1029	[39]
r_2	0.2978	0.2978	[39]
$S(0)$	11081000	11081000	[39]
$E(0)$	600	600	[39]
$I_1(0)$	410	410	[39]
$I_2(0)$	30	30	[39]
$R(0)$	2	2	[39]

Table 1. The values of various parameters in system (10).

γ	R_0	Equilibrium point P^*	Stability
0.8	1.895960	$P^* = (274924, 16012, 16322, 3477, 206732)$	P^* is GAS
0.85	2.056275	$P^* = (577132, 33883, 36328, 7289, 524608)$	P^* is GAS
0.9	2.223072	$P^* = (1215397, 70543, 79370, 15005, 1306965)$	P^* is GAS
0.95	2.396921	$P^* = (2566451, 145077, 170955, 30464, 3210473)$	P^* is GAS
1.0	2.578462	$P^* = (5431767, 295535, 364105, 61187, 7799401)$	P^* is GAS

Table 2. Endemic equilibrium point for different γ in the first set of values.

$$R_0 = \frac{S_0 \beta_1^\gamma p \epsilon^\gamma}{(\epsilon^\gamma + \mu^\gamma)(\mu^\gamma + \alpha^\gamma + r_1^\gamma)} + \frac{S_0 \beta_2^\gamma q \epsilon^\gamma}{(\epsilon^\gamma + \mu^\gamma)(\mu^\gamma + \alpha^\gamma + r_2^\gamma)}.$$

To optimize the analysis, we utilize the parameter settings in Table 1. Numerical computations provide the disease-free equilibrium values for different γ levels, which are systematically listed in Table 3.

Based on the information in the Table 2, we can plot the relationship between the order γ and the basic reproduction number R_0.

Figure 3 on the left represents the relationship between R_0 and γ under the first set of parameter values, while the graph on the right illustrates the same relationship under the second set of values. From the left graph, it can be observed that for $\gamma = 0.8, 0.85, 0.9, 0.95, 1$, the basic reproduction number $R_0 > 1$. According to Theorem 4.2, this implies that the endemic equilibrium P^* is globally asymptotically stable. Through further calculations, we can determine the specific endemic equilibrium and its stability for different γ values in the first set of parameters. Similarly, for the second set of values, the right graph shows that $R_0 \leq 1$ for all γ, indicating that the disease-free equilibrium P_0 is stable across different γ values.

In Tables 2 and 3, we calculated the endemic equilibrium point and disease-free equilibrium point, further verifying the correctness of the theoretical analysis.

Taking initial value are $S(0) = 11081000$, $E(0) = 600$, $I_1(0) = 410$, $I_2(0) = 30$, $R(0) = 2$, we can get a plot of $S(t)$, $E(t)$, $I_1(t)$, $I_2(t)$, and $R(t)$ over time in the first set of values.

From Fig. 4, it can be observed that the fractional-order parameter γ not only influences the dynamic behavior of the disease transmission model but also reflects the memory and nonlocal properties of fractional derivatives. Lower values of γ(such as $\gamma = 0.8$ and $\gamma = 0.85$) enhance the system's rapid decay characteristics, causing the number of infected individuals to decrease quickly, which indicates shorter memory effects. In contrast, higher values of γ(such as $\gamma = 0.95$ and $\gamma = 1$) strengthen the system's nonlocal characteristics, making the disease transmission and recovery processes slower and more prolonged. Fractional derivatives, by incorporating weighted memory of historical states, regulate the rate and scale of disease transmission, highlighting their unique advantage in describing complex dynamic systems and providing theoretical support for more precise modeling and control of disease spread.

Taking initial value are $S(0) = 11081000$, $E(0) = 600$, $I_1(0) = 410$, $I_2(0) = 30$, $R(0) = 2$ we can get a plot of $S(t)$, $E(t)$, $I_1(t)$, $I_2(t)$, $R(t)$ over time in the second set of values.

"*Fractional models required 1.5C2× more computation time than integer-order counterparts. Adaptive step sizing reduced this gap by 30% without sacrificing accuracy.*"
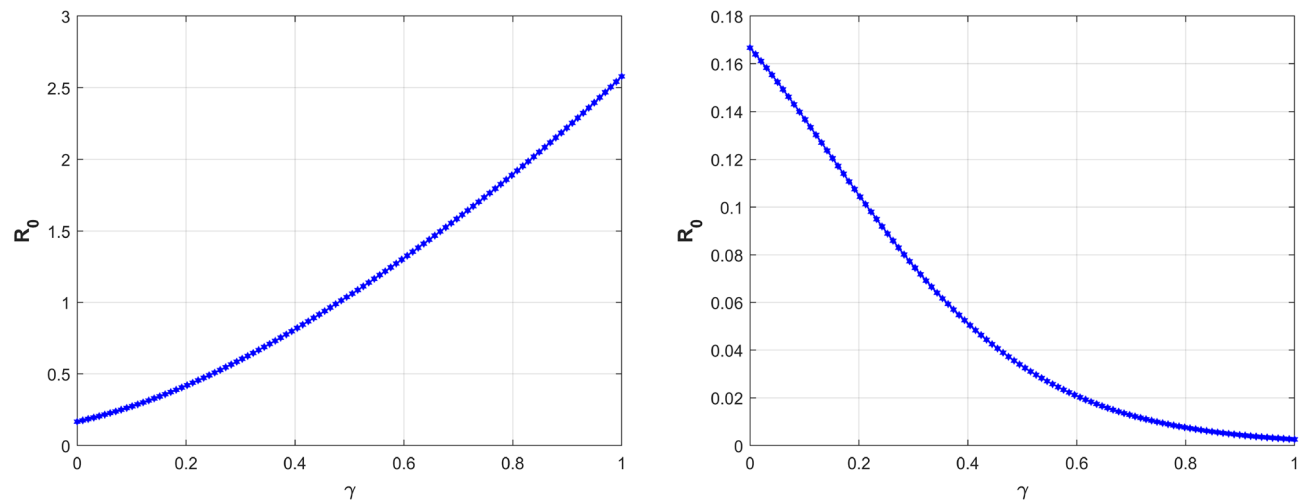
Fig. 3. Plot of R_0 versus γ for the first and the second set of values.

γ	R_0	Equilibrium point P_0	Stability
0.8	0.007548	$P_0 = (521244, 0, 0, 0, 0)$	P_0 is GAS
0.85	0.005795	$P_0 = (1186743, 0, 0, 0, 0)$	P_0 is GAS
0.9	0.004436	$P_0 = (2701915, 0, 0, 0, 0)$	P_0 is GAS
0.95	0.003386	$P_0 = (6151580, 0, 0, 0, 0)$	P_0 is GAS
1.0	0.002578	$P_0 = (14005602, 0, 0, 0, 0)$	P_0 is GAS

Table 3. Disease-free equilibrium point for different γ in the second set of values.

From Fig. 5, it can be observed that different fractional order parameters γ have a significant impact on the dynamic behavior of the system. From the E, I_1, I_2, and R plots, it is evident that the larger the order γ, the faster the changes occur, reflecting the memory and hereditary properties of fractional calculus. Lower γ values (e.g., $\gamma = 0.8$) prolong convergence due to stronger memory effects.

Through Figs. 4 and 5, we observed that when $R_0 > 1$, the number of infected individuals stabilizes at a positive equilibrium point, while when $R_0 < 1$, the number of infected individuals eventually converges to zero, which fully matches the theoretical analysis. In the figures, we respectively show the time evolution curves of susceptible S, exposed E, infected individuals (both symptomatic and asymptomatic), and recovered R under the first and second sets of parameter settings with different fractional order values.
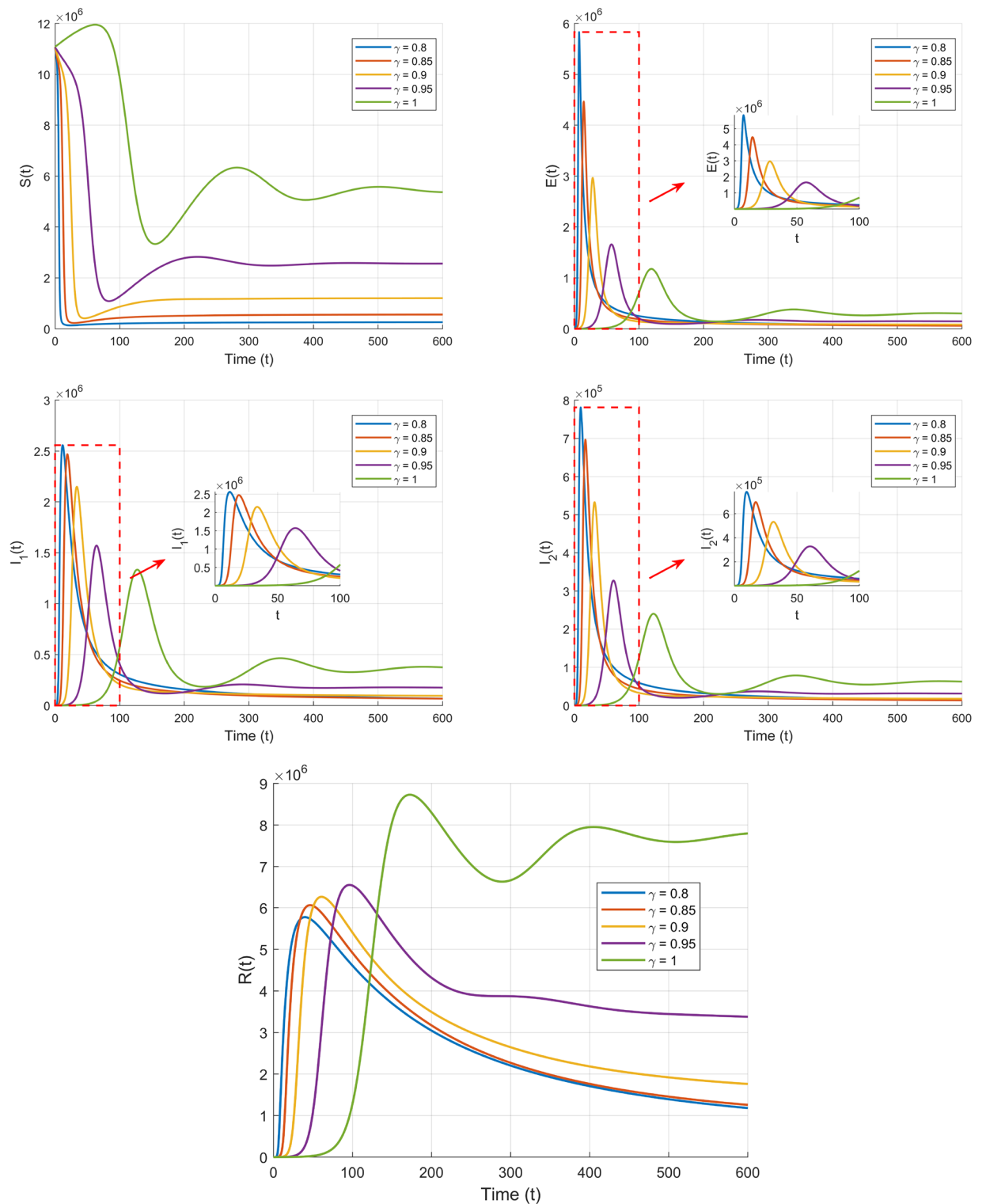
Through the above simulation, we observe that the fractional order parameter γ significantly influences the dynamic behavior of system (10). From the plots of $S(t)$, $E(t)$, $I_1(t)$, $I_2(t)$, and $R(t)$ with respect to t, under conditions where $R_0 < 1$ or $R_0 > 1$, it is clear that the rate of change in the curves for $\gamma < 1$ differs notably from those for $\gamma = 1$. This reflects the memory and hereditary characteristics intrinsic to fractional order systems. By tuning the fractional order parameter γ, the speed and duration of disease transmission can be effectively regulated, offering a more refined and accurate modeling framework for designing disease prevention and control strategies. *Memory effects imply that control measures (e.g., lockdowns) require earlier implementation to counteract historical transmission inertia.*

Conclusions

Many scholars have studied the dynamics of multi-disease coexistence[41], the impact of socio-economic factors on disease transmission[42], and virus transmission modeling incorporating deep learning and intervention measures[43]. Fantaye et al.[44] applied the ABC fractional derivative to study the transmission of coffee berry disease (CBD). These studies provide valuable references for the expansion and optimization of our model, particularly in characterizing complex disease transmission processes, optimizing model parameters, and improving predictive accuracy.

Although this paper proposes and analyzes an SEIR model with generalized infection rate based on Caputo fractional derivatives, enriching the theoretical framework of the classical model, there are still certain limitations. Firstly, although the generalized infection rate function is more general than the classical model, we assume that the function satisfies the separable variable condition, which limits the model's applicability to more complex infection rate functions. Secondly, this paper assumes the order of the fractional derivative to be constant, while in real epidemic dynamics, the memory effect of the system may vary over time, so it would be more reasonable to use variable-order fractional derivatives. Future research will consider more general $h(S, I)$ forms and the application of variable-order fractional derivatives. For future research directions,
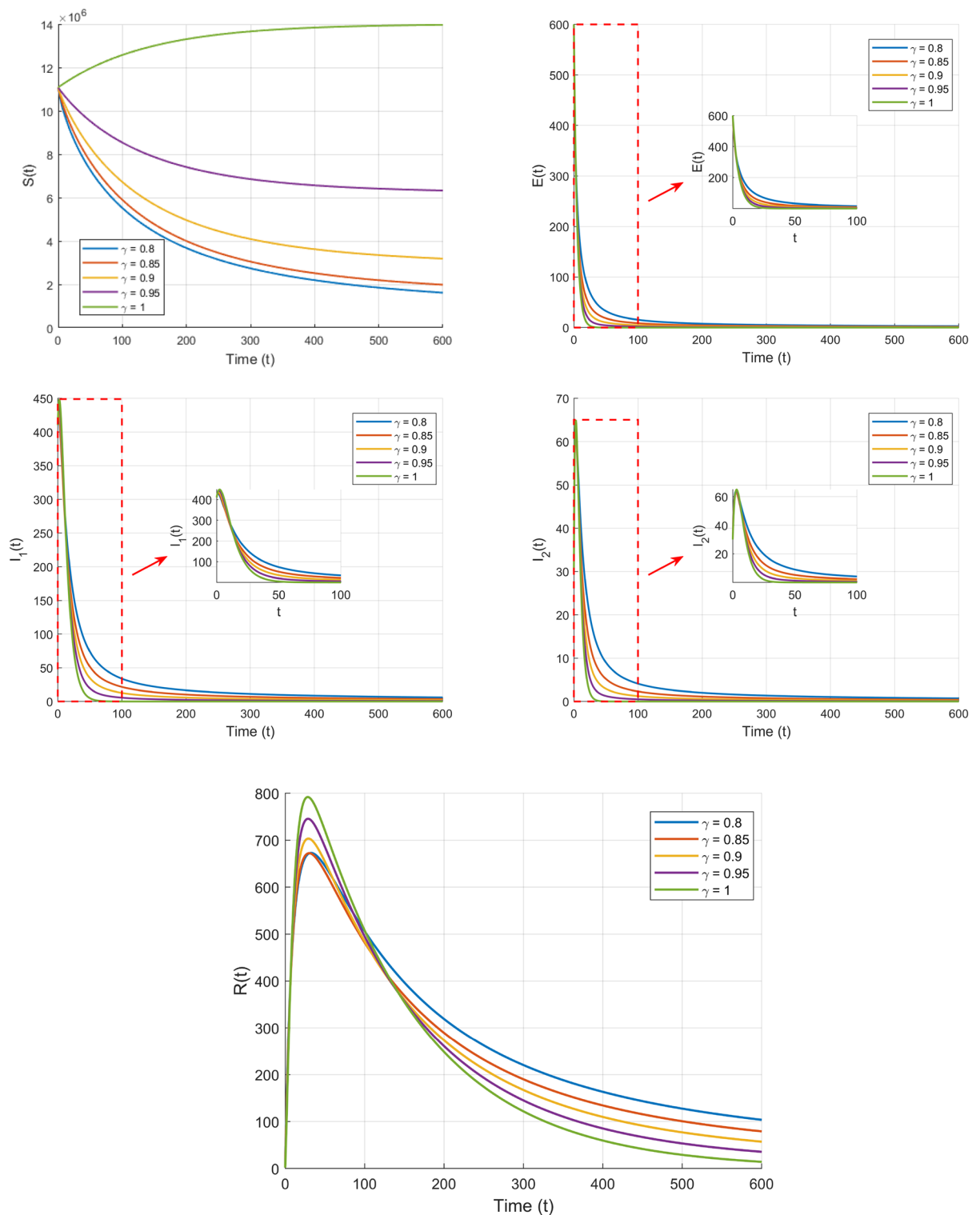
Fig. 4. Plot of $S(t), E(t), I_1(t), I_2(t), R(t)$ in terms of t.

the fractional-order model could dynamically capture the memory effects at different stages of the epidemic by introducing variable-order fractional derivatives, or better adapt to complex transmission environments by considering time-varying parameters and stochastic perturbations. Additionally, the model could be extended to a spatial fractional partial differential model to account for the impact of geographic heterogeneity, population movement, and other factors on epidemic transmission.

Fig. 5. Plot of $S(t), E(t), I_1(t), I_2(t), R(t)$ in terms of t.

Data availability
Data sharing not applicable to this article as no datasets were generated or analyzed during the current study.

References

1. Dobson, A. P. & Carper, E. R. Infectious diseases and human population history. *Bioscience* **46**(2), 115–126 (1996).
2. Spink, W. W. *Infectious Diseases: Prevention and Treatment in the Nineteenth and Twentieth Centuries* (University of Minnesota Press, 1978).
3. Duggan, A. T. et al. 17th Century variola virus reveals the recent history of smallpox. *Curr. Biol.* **26**, 3407–3412 (2016).
4. Platt, C. *King Death: The Black Death and its Aftermath in Late-medieval England* (Routledge, 2014).
5. Faruque, S. M. et al. Genetic diversity and virulence potential of environmental Vibrio cholerae population in a cholera-endemic area. *Proc. Natl. Acad. Sci. U.S.A.* **101**(7), 2123–8 (2004).
6. Hethcote, H. W. The mathematics of infectious diseases. *SIAM Rev.* **42**(4), 599–653 (2000).
7. Castillochavez, C. *Mathematical Models in Population Biology and Epidemiology* (Springer, 2012).
8. Kermack, W. O. & Mckendrick, A. G. A contribution to the mathematical theory of epidemics. *Proc. R. Soc. A Math. Phys. Eng. Sci.* **115**(772), 700–721 (1927).
9. Cooke, K. L. & Driessche, P. V. D. Analysis of an SEIRS epidemic model with two delays. *J. Math. Biol.* **35**(2), 240–260 (1996).
10. Wu, Y., et al. Agent transformation of Bayesian games. *IEEE Trans. Autom. Control* **67**(11), 5793–5808 (2021).
11. Guo, Y. et al. Set stability and set stabilization of Boolean control networks based on invariant subsets. *Automatica* **61**, 106–112 (2015).
12. Shi, X. et al. Fractals of interpolative Kannan mappings. *Fractal Fract.* **8**(8), 493 (2024).
13. Guo, Y., Wu, Y. & Gui, W. Stability of discrete-time systems under restricted switching via logic dynamical generator and STP-based mergence of hybrid states. *IEEE Trans. Autom. Control* **67**(7), 3472–3483 (2021).
14. Wang, X., Zhang, L. & Guo, J. Dynamics of a deterministic and stochastic susceptible-exposed-infectious-recovered epidemic model. *J. Nonlinear Model. Anal.* **5**(1), 24–53 (2023).
15. Oldham, K. & Spanier, J. *The Fractional Calculus Theory and Applications of Differentiation and Integration to Arbitrary Order* (Elsevier, 1974).
16. Kilbas, A. A. A., Srivastava, H. M. & Trujillo, J. J. Theory and applications of fractional differential equations. *North-Holland Math. Stud.* **2006**, 204 (2006).
17. Diethelm, K. & Ford, N. J. Analysis of fractional differential equations. *J. Math. Anal. Appl.* **265**(2), 229–248 (2002).
18. Atanackovic, T. M. et al. *Fractional Calculus with Applications in Mechanics: Vibrations and Diffusion Processes* (Wiley, 2014).
19. Monje, C. A. et al. *Fractional-Order Systems and Controls: Fundamentals and Applications* (Springer, 2010).
20. Ferdi, Y. Fractional order calculus-based filters for biomedical signal processing. In *Middle East Conference on Biomedical Engineering*, 73–76 (2011).
21. Laskin, N. Fractional quantum mechanics. *Phys. Rev. E* **62**(3), 3135 (2000).
22. Aguila-Camacho, N., Duarte-Mermoud, M. A. & Gallegos, J. A. Lyapunov functions for fractional order systems. *Commun. Nonlinear Sci. Numer. Simul.* **19**(9), 2951–2957 (2014).
23. Vargas-De-León, C. Volterra-type Lyapunov functions for fractional-order epidemic systems. *Commun. Nonlinear Sci. Numer. Simul.* **24**(1–3), 75–85 (2015).
24. Boukhouima, A. et al. Lyapunov functions for fractional-order systems in biology: Methods and applications. *Chaos Solitons Fractals* **140**, 110224 (2020).
25. Boukhouima, A. et al. Lyapunov functions and stability analysis of fractional-order systems. *Math. Anal. Infect. Dis.* **2022**, 125–136 (2022).
26. Yang, Y. & Xu, L. Stability of a fractional order SEIR model with general incidence. *Appl. Math. Lett.* **105**, 106303 (2020).
27. Almeida, R. Analysis of a fractional SEIR model with treatment. *Appl. Math. Lett.* **84**, 56–62 (2018).
28. Ahmad, Z. et al. A report on COVID-19 epidemic in Pakistan using SEIR fractional model. *Sci. Rep.* **10**(1), 9. https://doi.org/10.1038/s41598-020-79405-9 (2020).
29. Pan, W., Li, T. & Ali, S. A fractional order epidemic model for the simulation of outbreaks of Ebola. *Adv. Differ. Equ.* **2021**, 1–21 (2021).
30. Rezapour, S. & Mohammadi, H. A study on the AH1N1/09 influenza transmission model with the fractional Caputo-Fabrizio derivative. *Adv. Differ. Equ.* **2020**, 1–15 (2020).
31. Chen, Y. et al. Review of fractional epidemic models. *Appl. Math. Model.* **97**(4), 281–307 (2021).
32. Podlubny, I. *Fractional Differential Equations: An Introduction to Fractional Derivatives, Fractional Differential Equations, to Methods of Their Solution and Some of Their Applications* (Elsevier, 1998).
33. Matignon, D. Stability results for fractional differential equations with applications to control processing. *Comput. Eng. Syst. Appl.* **2**(1), 963–968 (1996).
34. Kong, Q. *A Short Course in Ordinary Differential Equations* (Springer, 2014).
35. Li, Y., Chen, Y. Q. & Podlubny, I. Stability of fractional-order nonlinear dynamic systems: Lyapunov direct method and generalized Mittag-Leffler stability. *Comput. Math. Appl.* **59**(5), 1810–1821 (2010).
36. Odibat, Z. M. & Shawagfeh, N. T. Generalized Taylor's formula. *Appl. Math. Comput.* **186**(1), 286–293 (2007).
37. Dreessche, P. & Watmough, J. Reproduction numbers and sub-threshold endemic equilibria for compartmental models of disease transmission. *Math. Biosci.* **180**(1–2), 29–48 (2002).
38. Berhe, H. W., Makinde, O. D. & Theuri, D. M. Parameter estimation and sensitivity analysis of dysentery diarrhea epidemic model. *J. Appl. Math.* **2019**(1), 8465747 (2019).
39. Xia, W. et al. When will be the resumption of work in Wuhan and its surrounding areas during COVID-19 epidemic A data-driven network modeling analysis. *Scientia Sin. Math.* **50**(7), 969–978 (2020).
40. Chen, M. et al. The introduction of population migration to SEIAR for COVID-19 epidemic modeling with an efficient intervention strategy. *Inf. Fus.* **64**, 252–258 (2020).
41. Omame, A. et al. Dynamics of Mpox in an HIV endemic community: A mathematical modelling approach. *Math. Biosci. Eng.* **22**(2), 225–259 (2025).
42. Ullah, M. A. et al. Analysis and interpretation of a novel malaria transmission mathematical model with socioeconomic structure. *Nonlinear Dyn.* **2024**, 1–20 (2024).
43. Mustafa, N., Rahman, J. U. & Omame, A. Modelling of Marburg virus transmission dynamics: A deep learning-driven approach with the effect of quarantine and health awareness interventions. *Model. Earth Syst. Environ.* **2024**, 1–21 (2024).
44. Fantaye, A. K. Fractional order for the transmission dynamics of coffee berry diseases (CBD). *Eur. J. Appl. Math.* **2024**, 1–18 (2024).

Author contributions

All the authors have made equally contributions to the publication of this article. All authors read and approved the final manuscript.

Funding

Declarations

Competing interests
The authors declare no competing interests.

Additional information
Correspondence and requests for materials should be addressed to S.X.

Reprints and permissions information is available at www.nature.com/reprints.

Publisher's note Springer Nature remains neutral with regard to jurisdictional claims in published maps and institutional affiliations.